Perspective Carbon Future

Spatiotemporal regulation of renewable energy via sustainable carbon-cycle fuels

Xiaoyu Liang[1], Hao Xiong[1] ✉, Chenxi Zhang[1,2,3] ✉, and Fei Wei[1,2,3] ✉

[1]Beijing Key Laboratory of Green Chemical Reaction Engineering and Technology, Department of Chemical Engineering, Tsinghua University, Beijing 100084, China.
[2]Ordos Laboratory, Ordos 017000, China.
[3]Institute for Carbon Neutrality, Tsinghua University, Beijing 100084, China.

Carbon Future 2026, 3, 9200090 https://doi.org/10.26599/CF.2026.9200090

Received: June 2, 2026; Revised: September 16, 2026; Accepted: September 17, 2026

✉ Address correspondence to Fei Wei, wf-dce@tsinghua.edu.cn; Chenxi Zhang, cxzhang@tsinghua.edu.cn; Hao Xiong, xionghao@mail.tsinghua.edu.cn

Just Accepted

Abstract:

Industrialization has driven intensive exploitation of fossil carbon resources, resulting in surging atmospheric CO_2 concentrations. Restoring global carbon cycle balance now demands effective decarbonization strategies. Yet despite rapid growth in renewable energy, spatiotemporal mismatches between supply and demand prevent electricity from fully displacing fossil fuels. Hydrogen energy faces similar obstacles, including variable production costs and geographic imbalances between sources and consumers. Here, we propose an integrated pathway for synthesizing sustainable carbon-cycle fuels that enables long-duration, high-capacity spatiotemporal regulation of renewable energy. This approach couples renewable electricity-driven water electrolysis for green hydrogen production with CO_2 captured via direct air capture (DAC) or industrial carbon capture, utilization, and storage (CCUS) technologies. The captured CO_2 and hydrogen then undergo photosynthesis-inspired catalytic conversion to yield carbon-neutral liquid fuels. This strategy leverages advanced catalysis, promotes carbon cycling, and remains compatible with existing refining infrastructure. Although challenges persist in catalyst longevity, system efficiency, and production economics, continued technological progress should enable large-scale chemical storage of renewable energy—offering a viable pathway toward global deep decarbonization.

Keywords: Renewable energy; CO_2 hydrogenation; Deep decarbonization; Energy storage; Green hydrogen

1. Introduction:

Carbon, a fundamental element of Earth's life-support system, links the inorganic and organic realms through complex biogeochemical cycling. It is exchanged among major reservoirs—including the atmosphere, terrestrial biosphere, oceans, sediments, and Earth's interior—via diverse pathways (Fig. 1)[1-3]. The carbon cycle comprises two distinct components: a fast (biological) cycle and a slow (geological) cycle. The fast cycle operates within the biosphere over years to decades. Through photosynthesis, plants convert atmospheric CO_2 into organic carbon within the terrestrial biosphere. This organic carbon is then returned to the atmosphere as CO_2 or CH_4 via respiration, microbial decomposition, root metabolism, and soil fauna activity[4, 5]. The slow cycle, by contrast, involves deep carbon exchanges across the lithosphere, atmosphere, and hydrosphere through sedimentation, tectonic activity, and other geological processes, unfolding over millions of years[6, 7]. Without anthropogenic interference, carbon fluxes between these reservoirs maintain dynamic equilibrium and relatively stable global carbon levels[8].

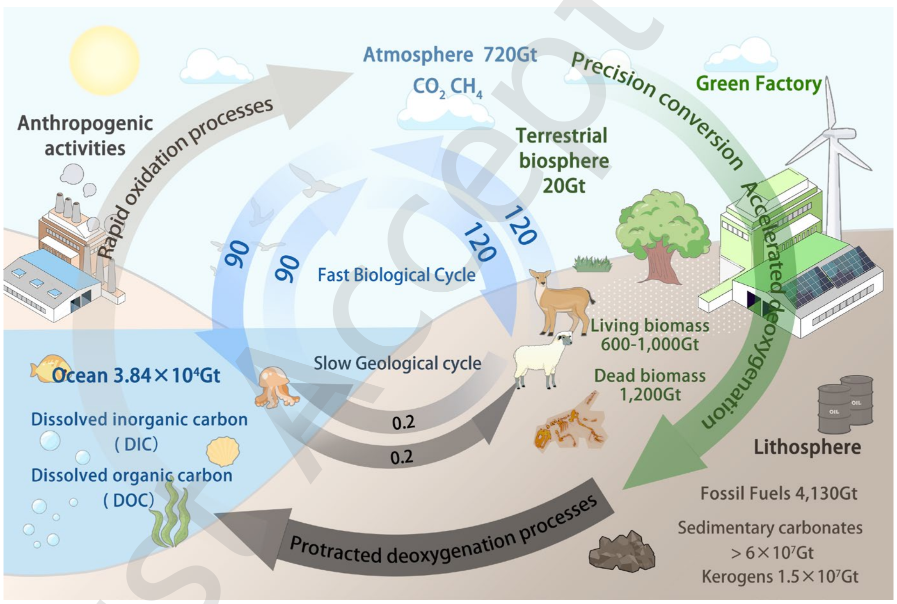

Fig. 1. Sustainable carbon cycle model in nature driven by precise, accelerated deoxygenation processes in green chemical industries.

The industrialization-triggered energy paradigm shift initiated exploitative extraction of fossil carbon from geological reservoirs. Between 1750 and 2020, anthropogenic activities cumulatively released approximately 450 ± 20 Gt of fossil carbon into the atmosphere—comparable to the total carbon stored in all terrestrial biomass—marking the first time in history that human-induced disturbances have surpassed natural geological forces in the global carbon cycle[9-11] (Fig. 2a). This trans-temporal carbon transfer is largely irreversible: carbon stored over millions of years in sedimentary rocks via the slow carbon cycle is now being released into the atmosphere at a rate of 8–10 Gt C per year.

However, Earth's intrinsic negative feedback mechanisms—including silicate weathering and oceanic carbonate pumps—operate on timescales of 10^3–10^5 years, far exceeding the century-scale pace of industrial emissions (Fig. 1). Consequently, atmospheric CO_2 concentrations surged from pre-industrial levels of 280 ppm to 424 ppm in 2023[12] (Fig. 2b), disrupting the intergenerational

Just Accepted

equilibrium of the carbon system and triggering cascading environmental consequences. The enhanced greenhouse effect has attracted particular attention: global mean surface temperature in 2024 rose 1.55 ± 0.13 °C above pre-industrial levels (1850–1900 baseline), approaching the 1.5 °C threshold set by the Paris Agreement[13] .

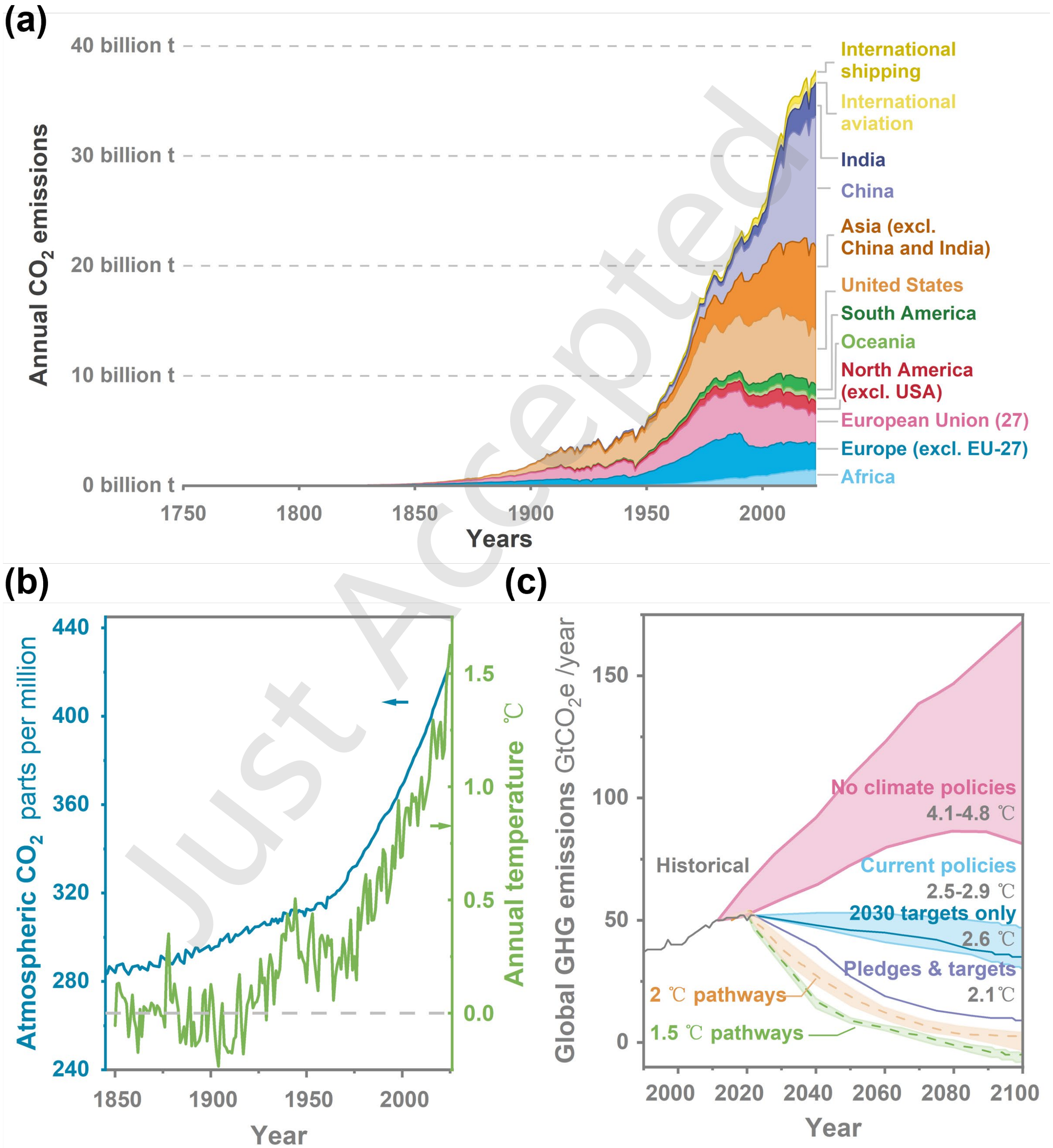

Just Accepted

Fig. 2. Exploitative extraction of geological carbon reserves following the Industrial Revolution. (**a**) Regional anthropogenic CO_2 emissions from 1750 to 2020, showing cumulative emissions of approximately 450 ± 20 Gt—comparable to Earth's entire terrestrial biomass carbon

stock[11]. (**b**) Atmospheric CO_2 concentration since 1850, rising from ~280 ppm to 424 ppm by 2023, with corresponding global mean surface temperature changes. (**c**) Impact of multilevel environmental policies on projected global greenhouse gas (GHG) emissions.

In response to this carbon imbalance crisis, a multilayered policy framework has been developed globally (Fig. 2c). Under its "Fit for 55" package, the EU aims to cut emissions by 55% from 1990 levels by 2030 through renewable energy expansion, tighter industrial emission limits, and the EU Emission Trading System spanning power and aviation sectors[14]. The United States has leveraged the Inflation Reduction Act to accelerate clean energy innovation and deployment via tax credits and R&D investments. China's "Carbon Peaking and Carbon Neutrality" initiative established a comprehensive policy network encompassing renewable energy planning, industrial efficiency upgrades, and a nationwide carbon market. Nevertheless, International Energy Agency (IEA) projections suggest that under current trajectories, global warming could reach 2.5–2.9 °C by 2100—well above the Paris Agreement target[15].

To achieve transformative carbon mitigation, a dual-paradigm shift is required: first, replacing fossil fuels with alternative energy carriers (e.g., wind, solar, electricity, and heat) to halt rapid release of geological carbon while minimizing perturbations to existing biological and geological carbon cycles; second, developing deoxygenation pathways with enhanced water-use efficiency and accelerated kinetics to overcome the water dependency of photosynthesis in biological cycle and the rate-limiting steps of geological cycles. This would establish a fast artificial deoxygenation-carbon pathway, ultimately forming a novel closed carbon loop.

The first paradigm, based on renewable electricity and electricity-based energy storage, has achieved remarkable progress in technologies such as batteries and pumped hydro storage, enabling renewable power balancing. However, their limited energy density, resource requirements, and geographical constraints remain challenges for long-duration, large-scale, and cross-regional energy storage. Meanwhile, chemical energy carriers based on artificial carbon-cycle pathways have emerged as a promising complement by storing renewable energy in stable chemical bonds while enabling carbon recycling. Nevertheless, their technological readiness, economic viability, and scalability require further evaluation. Therefore, a comprehensive understanding of the advantages and limitations of both paradigms is essential for identifying optimal pathways toward deep decarbonization. This study systematically evaluates the technical readiness, energy-storage economics, and scalability of both paradigms to identify optimal deep decarbonization pathways.

2. Renewable clean energy

2.1 Rapid development of renewable clean energy

The pursuit of alternative clean energy sources has garnered significant global attention in recent years amid the ongoing energy consumption transition. Electricity has increasingly emerged as a dominant energy carrier, driven by growth in electricity-intensive clean energy manufacturing,

Just Accepted

rising air conditioning usage, widespread electric vehicle (EV) adoption, and expansion of data centers and 5G infrastructure.

Global renewable power generation has experienced remarkable growth (Fig. 3a). Over the past decade, renewable electricity generation increased consistently, with an additional 858 TWh generated in 2024 alone, accounting for 40.9% of global electricity production. By 2024, global installed renewable capacity reached 4,448 GW, with 585 GW added that year. This represented 92.5% of total newly installed capacity and achieved a record annual growth rate of 15.1%.[16, 17] Solar and wind power have been the primary drivers of this expansion.[18, 19]

China has emerged as a pivotal force in the global renewable energy landscape. Between 2014 and 2024, China's installed wind power capacity increased sixfold (from ~96 GW to 521 GW), while solar power capacity expanded thirty-twofold (from ~28 GW to 887 GW) (Fig. 3b-c). In 2023, China's renewable energy installations exceeded 50% of total power capacity for the first time, reaching 1.45 billion kilowatts (Fig. 3d)[20]. By 2024, China generated 3.46 trillion kWh of renewable electricity, representing 35% of total output[21]. China's global impact is also striking: it accounted for 60% of newly added renewable capacity worldwide in 2024[19], contributed 50% of global solar photovoltaic additions, and supplied 60% of exported wind turbine equipment.

This rapid growth has driven significant reduction in solar power generation costs, catalyzed by economies of scale, favorable policies, and continuous technological advances in Passivated Emitter and Rear Cell(PERC), Tunnel Oxide Passivated Contact (TOPCon), and Heterojunction Technology(HJT) solar cells. Empirical studies reveal a strong learning curve in solar photovoltaics[22-27], with a learning rate of 23.5%[28-30]—meaning that photovoltaic module prices decrease by 23.5% with every doubling of global cumulative installed capacity (Fig. 3e). Consequently, commercial photovoltaic module prices dropped from USD 6.41/W in 2000 to USD 0.31/W in 2023, significantly lowering the levelized cost of electricity (LCOE), defined as the lifetime-average system-level cost per unit of electricity generated, including generation, storage, transmission, and distribution [31, 32]. In 2024, the global average LCOE of fixed-tilt photovoltaic systems declined to USD 66/MWh. In China, the global center of photovoltaic (PV) manufacturing, LCOE has fallen to 0.15-0.24 RMB/kWh, below coal-fired electricity generation costs (0.30-0.35 RMB/kWh), marking a historic shift in solar power's economic competitiveness[33].

Wind power has also demonstrated significant cost improvements[32]. Through aerodynamic blade optimization (e.g., adaptive airfoil designs), turbine scaling, and intelligent operation and maintenance systems, the global weighted-average LCOE for onshore wind dropped from USD 0.111/kWh in 2010 to USD 0.033/kWh in 2023, signaling growing economic viability[34].

Just Accepted

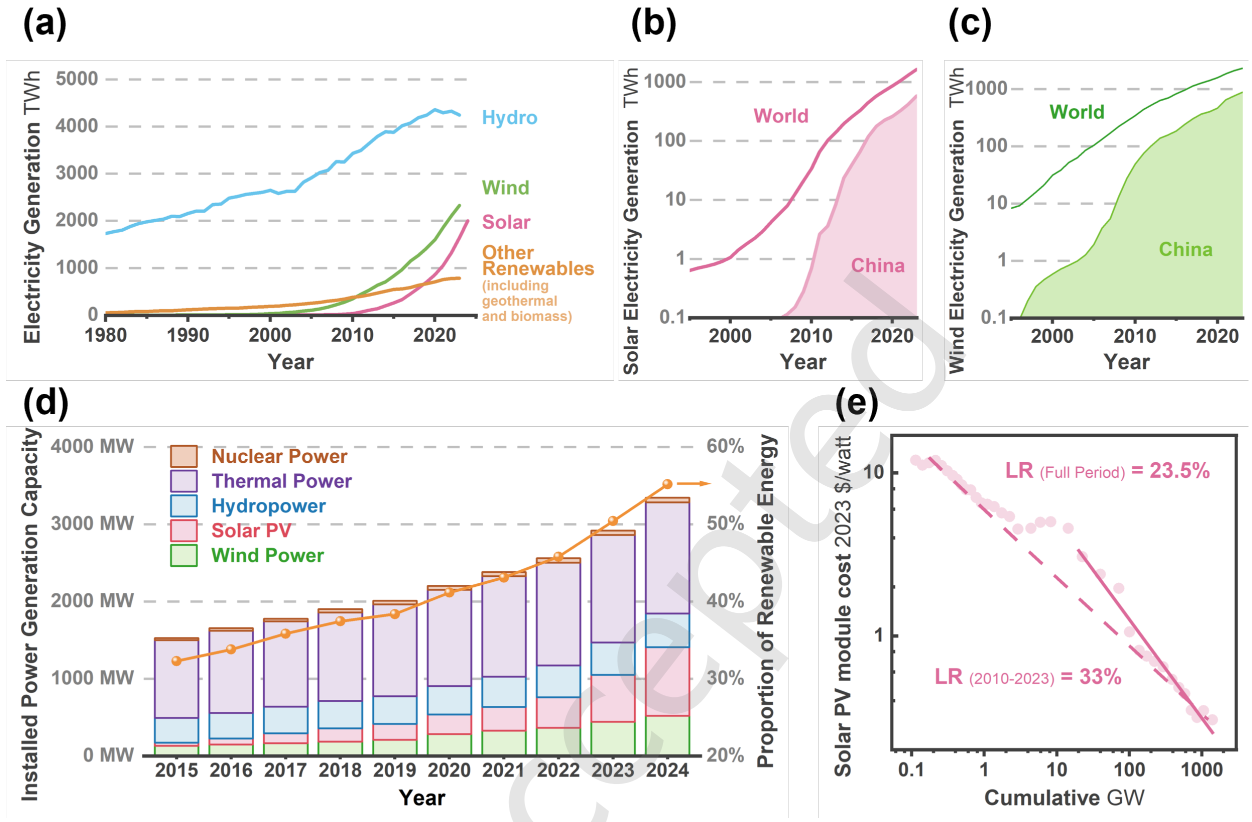

Fig. 3. Rapid development of renewable clean energy. (**a**) Growth trends in installed capacity for hydropower, wind, solar, and other renewable energy sources globally over the past four decades. (**b-c**)Global and China's growth trends in solar (**b**) and wind (**c**) electricity generation over the past four decades. (**d**) China's renewable energy installed capacity growth over the past decade, with wind and photovoltaic capacities increasing 6-fold and 32-fold, respectively; in 2023, renewables exceeded 50% of total installed capacity. (**e**) Learning curve effect on photovoltaic electricity generation costs.

2.2 Spatial-temporal mismatch between renewable electricity supply and demand

Despite rapid renewable energy advancement, relying on electricity as the primary vector for energy transition faces multiple structural challenges. First, the rising share of electricity is constrained by the gap between total energy consumption and power generation capacity. China's total energy consumption reached 5.96 billion tons of standard coal equivalent in 2024, while total electricity production stood at 10.1 trillion kWh—equivalent to only 1.24 billion tons of standard coal— only meeting approximately 20% of overall energy demand (Fig. 4a)[21]. This disparity highlights near-term limitations in electricity's ability to fully replace direct fossil fuel consumption.

Second, renewable energy's inherent intermittency increasingly conflicts with continuous electricity demand. In China, the average annual effective utilization hours for wind and solar PV are approximately ~2,100 and 1,250 hours respectively[35, 36], while the power system must ensure reliable supply for 8,760 hours yearly (Fig. 4b). This temporal mismatch becomes particularly critical under extreme weather. For example, drought in India during August 2024

Just Accepted

caused hydropower output to decline sharply, forcing coal-fired power to surge to 66.7% of the energy mix—revealing the vulnerability of renewable energy to meteorological fluctuations.

Due to diurnal variation in solar irradiance, renewable power generation typically peaks at midday but drops sharply at night, necessitating support from conventional or alternative power sources. Subtracting real-time renewable output from total electricity demand yields the net load curve, a metric reflecting operational stress on the power grid. This curve, colloquially termed the “duck curve” due to its shape, poses increasing challenges as solar capacity expands. As shown in Fig. 4c, California's power system demonstrates deepening midday demand troughs and even negative net loads during extreme periods, demanding advanced energy storage technologies to stabilize the grid[37, 38]. Currently, California flexibly meets its daily electricity demand by integrating solar, wind, hydro, and nuclear power, supplemented by battery storage and electricity imports/exports(Fig. 4d).[39]

On longer timescales—monthly and seasonal—the cyclical nature of wind and solar power continues to cause supply-demand mismatches (Fig. 4e)[40], necessitating seasonal load-balancing mechanisms for grid stability. These phenomena underscore the critical importance of developing electricity systems with temporal flexibility to absorb and utilize renewable energy efficiently while maintaining reliability.

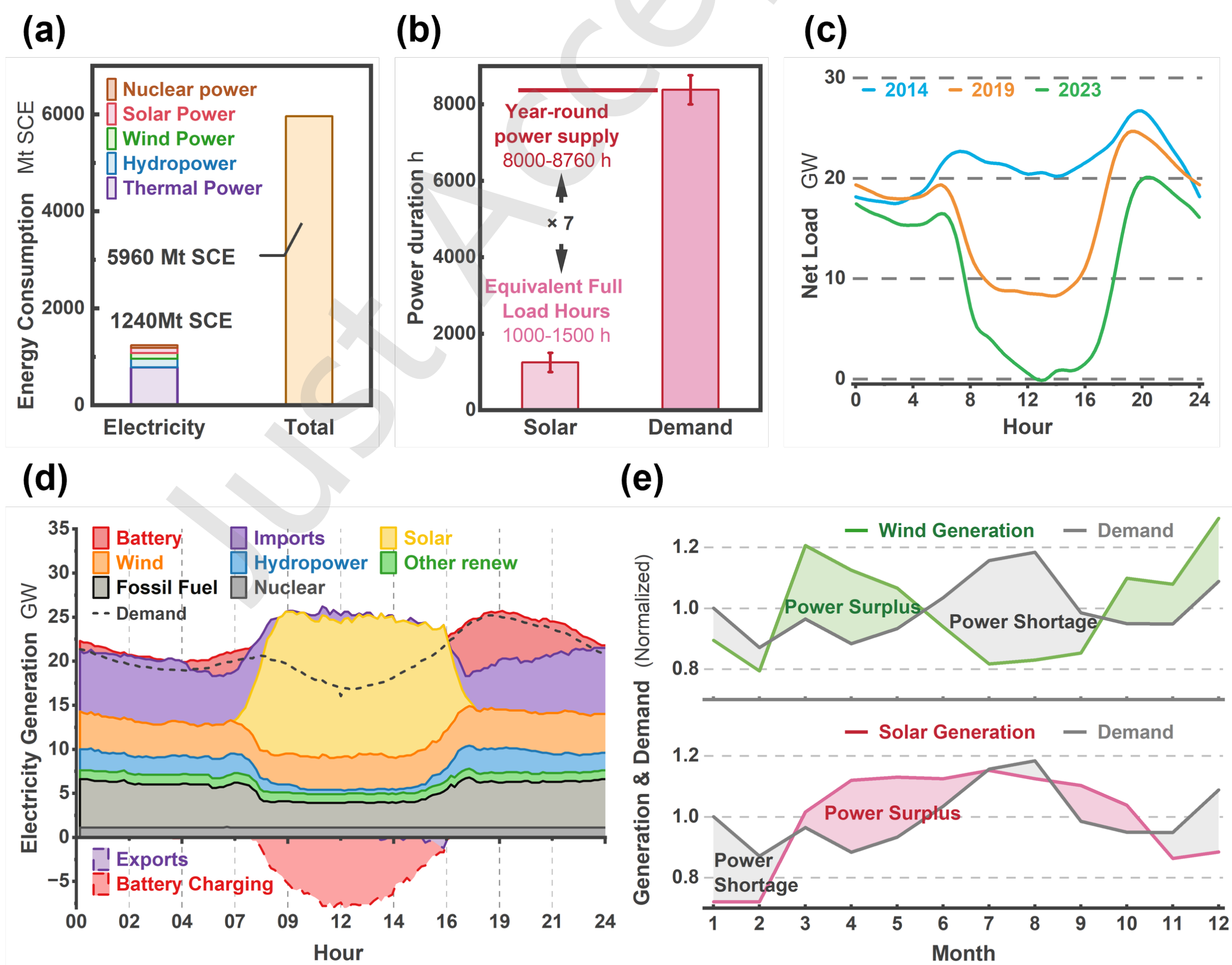

Fig. 4. Supply-demand mismatch in renewable energy systems caused by temporal imbalances. (**a**) Current electricity share in the overall energy system accounts for only 20% of total consumption. (**b**) Mismatch between annual effective utilization hours of wind and solar generation and electricity demand patterns. (**c**) Net load curve illustrating grid supply pressure due to daily solar radiation variations. (**d**) California's electricity generation breakdown by source on October 26, 2025[39] (**e**) Monthly and seasonal fluctuations in wind and solar generation creating supply-demand mismatches; seasonal peak-shaving measures are urgently needed.

Beyond temporal imbalance, electricity exhibits pronounced geospatial heterogeneity, which imposes higher demands on power storage and long-distance transmission infrastructure[41]. In China, western regions possess abundant wind and solar resources, contributing a disproportionately large share of national renewable capacity yet exhibiting relatively low electricity consumption. Eastern provinces, characterized by dense populations and robust economic activity, face high demand but limited renewable potential. Fig. 5a demonstrate the relationship between electricity production and consumption across provinces, as well as prevailing electricity transmission patterns. When China is divided by the Hu Line (the "Heihe–Tengchong Line", a demographic boundary), this spatial mismatch becomes even more apparent: electricity resources concentrate in the west, while demand centers lie predominantly in the east (Fig. 5b)[42]. This necessitates long-distance transmission from resource-rich regions to high-demand load centers, significantly increasing the average transmission distance.

Given the intermittent nature of renewable generation and the spatial decoupling between energy supply and demand, storage and transmission costs have become crucial components in renewable electricity economics. Studies show that when considering full lifecycle costs—including generation, storage, transmission, and distribution—the levelized cost of electricity (LCOE) may increase by 2- to 30-fold depending on distance and system configuration (Fig. 5c)[43-45].

Notably, with the advancement of renewable energy production, storage, and transportation, there is growing recognition that issues such as supply inadequacy, intermittency, and variability of renewable energy are largely localized. On a global scale, renewable energy reserves are remarkably substantial. Globally interconnectable solar and wind generation potential reaches 237 $\times 10^3$ TWh per year—approximately three times the projected electricity demand for 2050[46]. Furthermore, mid- and high-altitude wind resources above 300 meters, characterized by high speed, stable direction, and high energy density, possess a theoretical reserve capable of meeting global demand more than a hundred times over[47]. However, technological limitations have prevented extensive exploitation. These observations indicate that the core challenge for renewable energy substitution lies not in reserves but in establishing efficient, responsive regional—or even global—interconnections that enable flexible demand matching. Therefore, identifying intermediate energy forms offering superior economics in storage, transportation, and end-use becomes crucial.

Just Accepted

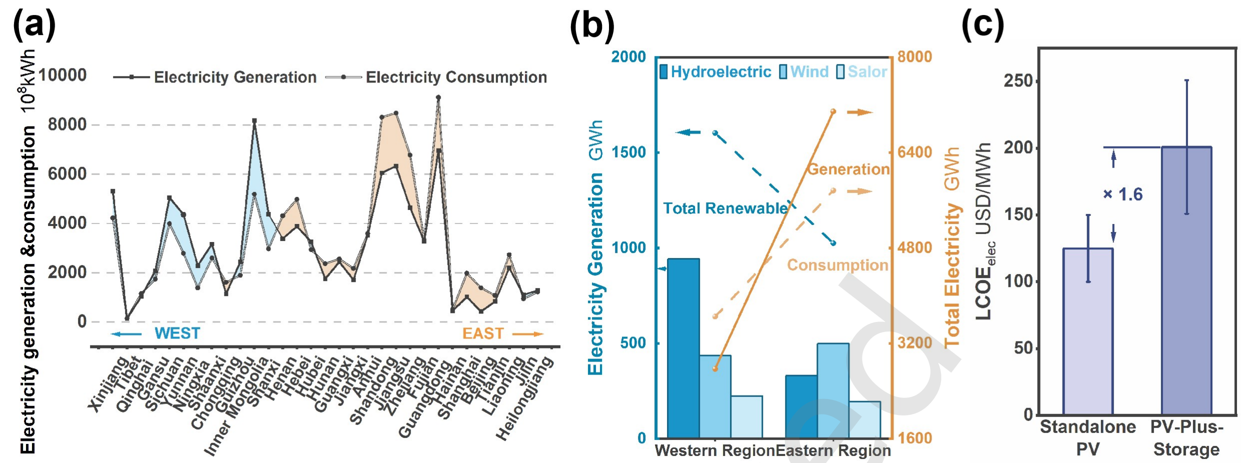

Fig. 5. Spatial distribution imbalances of renewable energy resources in China. (**a**) Provincial electricity generation, consumption, and inter-regional transmission relationships. (**b**) Regional mismatch between electricity resources and demand in western and eastern China. (**c**) Average levelized cost of electricity (LCOE), accounting for full life-cycle factors including production, storage, transportation, and distribution costs.

2.3 Hydrogen as a key carrier of zero-carbon energy

As a crucial carrier in a zero-carbon energy system, hydrogen has emerged as a key direction in the global energy transition, owing to its high gravimetric energy density (142 MJ/kg) and environmentally benign combustion product—pure water. Depending on production-associated carbon footprint, hydrogen is typically categorized as grey (fossil fuel-derived), blue (fossil fuel-derived with carbon capture and storage, achieving 60–80% emission reductions), or green (water electrolysis powered by renewable energy, near-zero emissions).[48]

In 2023, global hydrogen demand reached 97 million tons, with grey hydrogen supplying the majority. Low-carbon hydrogen (blue and green) production remained under 1 million tonnes annually, indicating minimal presence in the global energy mix (Fig. 6a).[49] According to IEA projections, meeting Paris Agreement climate goals requires replacing 30% of grey hydrogen demand with low-carbon alternatives by 2030. By 2050, grey hydrogen must be completely phased out, requiring approximately 690 million tons of low-carbon hydrogen annually—of which green hydrogen is expected to constitute ~70%[50]. By 2024, global installed electrolysis capacity reached 2.3 GW, an eightfold increase from 2020, with China accounting for 46% of new capacity.[51] Projections suggest global annual electrolyzer installation capacity could reach 9.3 GW by 2027, with China contributing 7.3 GW (~80% of global additions).[52]

The current levelized cost of hydrogen (LCOH) for green hydrogen comprises three primary components: electrolyzer depreciation (7–30%), electricity costs (50–70%), and operation and maintenance (O&M) costs (10–20%) (Fig. 6b).[53] Substantial potential exists for cost reduction (Fig. 6d)[54]. With technological advancement, electrolysis capital costs are projected to decline at a 16% learning rate (Fig. 6c).[55] As of 2024, electricity pricing remains the dominant factor in green hydrogen economics. Modeling indicates that when renewable electricity prices fall below RMB 0.2/kWh, green hydrogen production costs can drop below RMB 15/kg, achieving cost-competitiveness with blue hydrogen (RMB 12–18/kg) (Fig. 6e). In northwest China, integrated

Just Accepted

wind–solar–hydrogen projects have achieved green hydrogen costs in the range of RMB 15–20/kg (approximately twice the price of grey hydrogen) in 2024, with expectations of reaching under RMB 12/kg by 2026, thus achieving cost parity with grey hydrogen.[56]

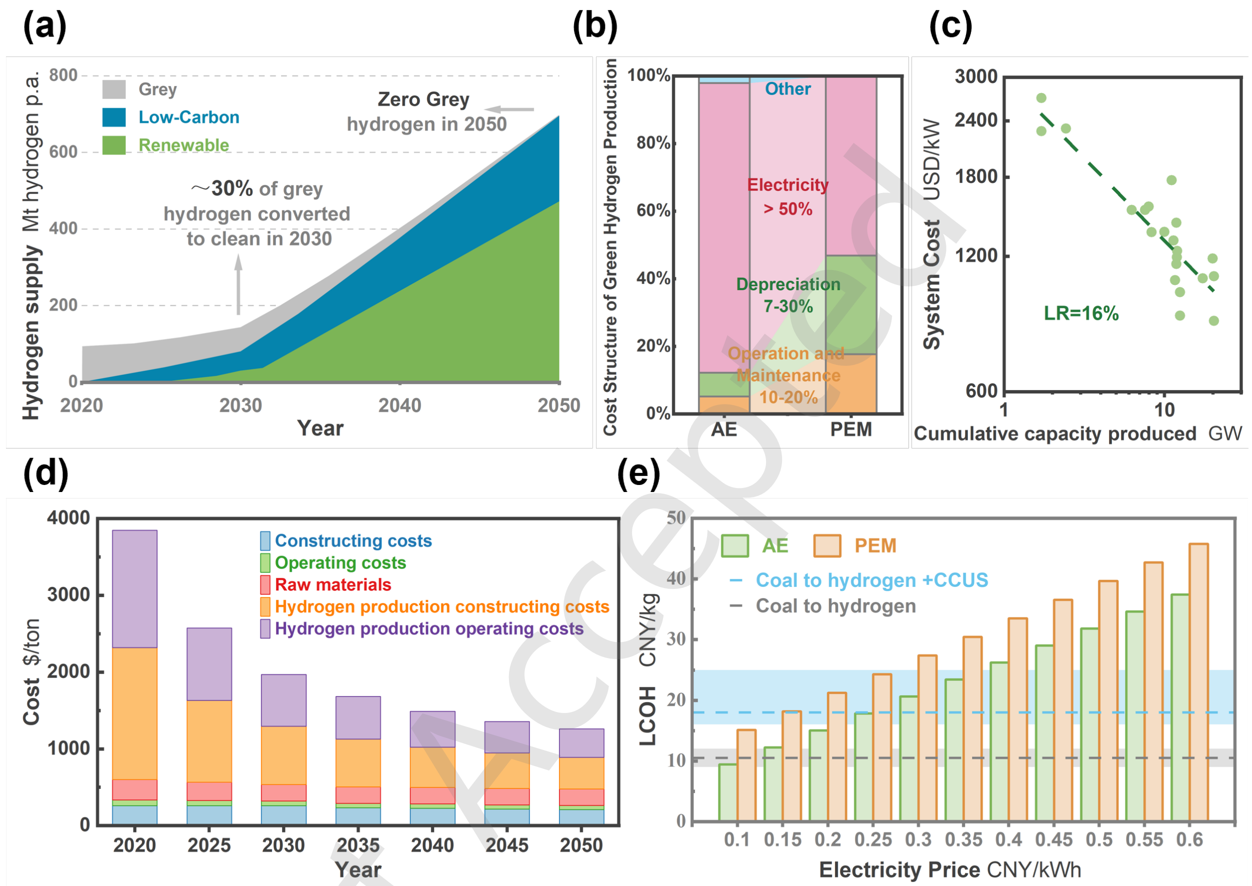

Fig. 6. Hydrogen as a key carrier of zero-carbon energy. (**a**) Growth trends in different hydrogen supply types. (**b**) Cost components of Alkaline Electrolysis (ALK) and Proton Exchange Membrane (PEM) hydrogen production technologies. (**c**) Learning curve effect on electrolyzer costs. (**d**) Green hydrogen cost variations as influenced by electricity prices. (**e**) Impact of electricity price on the Levelized Cost of Hydrogen (LCOH) for green hydrogen.

Just Accepted

Beyond high production costs, large-scale green hydrogen deployment is severely limited by transportation expenses. Pronounced geographical mismatch between production sites and demand centers makes storage and transport unavoidable—accounting for over 40% of final hydrogen price (Fig. 7a). These costs rise considerably with distance, representing a key obstacle to a sustainable hydrogen economy.

Hydrogen is transported primarily in three forms: high-pressure gas, cryogenic liquid, and pipelines (Fig. 7b)[57]. High-pressure gaseous hydrogen—typically delivered by tube trailers at 20 MPa—is the dominant mode, covering 92% of shipments, though it remains economical only under 300 km. Liquid hydrogen, liquefied at –253°C, suits medium- to long-distance transport

(500–1000 km), yet high liquefaction energy costs remain a major drawback. Pipeline transport generally offers the lowest levelized transportation cost for long-distance (>400 km) and large-scale (>100,000 tons/year) delivery, with transportation costs incorporating annualized capital investment and operating expenses, but faces technical and infrastructural hurdles alongside stricter safety and material requirements due to hydrogen's inherent properties.Notably, hydrogen's low volumetric energy density—about 12.7 MJ/m³ under standard conditions, roughly one-third that of natural gas (39 MJ/m³)—combined with lower pipeline flow velocities results in significantly reduced transport efficiency compared with conventional natural gas systems. Although China has accelerated its pipeline network development—with over 7,000 km of pipelines under development by March 2025 and growing market investment—core challenges in efficiency and safety remain (Fig. 7c). Overcoming these bottlenecks will require fundamental technological advances to enable a future integrated and large-scale hydrogen transport infrastructure.

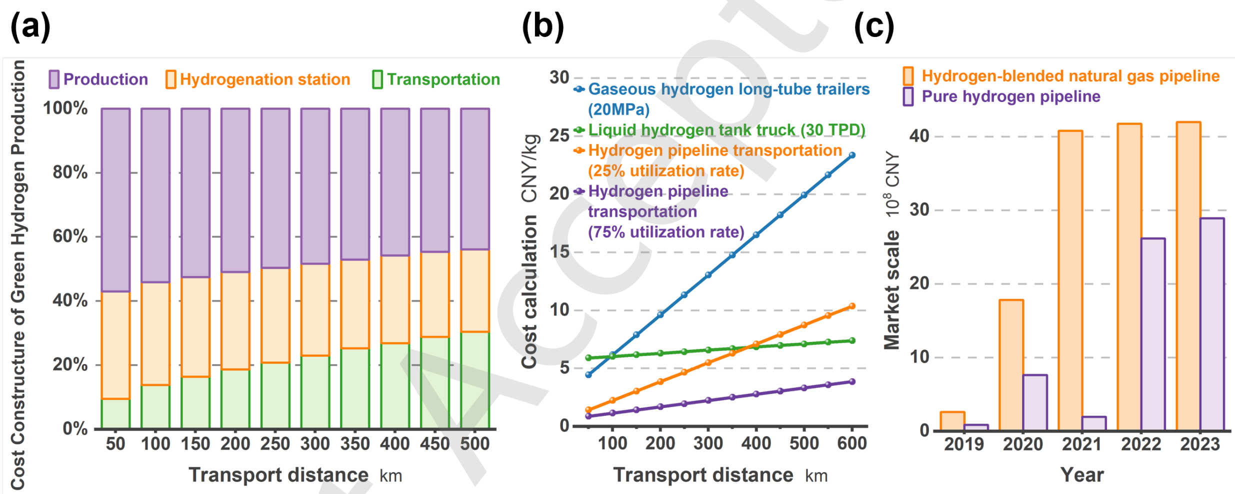

Fig. 7. Spatial asymmetry of supply and demand in the green hydrogen industry. (**a**) Cost composition of green hydrogen across different transport distances. (**b**) Comparative costs of green hydrogen via different transportation methods at varying distances. (**c**) Market size of hydrogen pipelines in China.

3. Hydrocarbon Energy Storage

3.1 Energy-dense hydrocarbon liquids

As chemical energy carriers, hydrocarbons maintain an irreplaceable position in global energy systems owing to well-established storage and transportation infrastructure and high energy density [58] (Fig. 8a). Common energy-type hydrocarbons include methane (50–55 MJ/kg), methanol (19.9 MJ/kg), gasoline (46.4 MJ/kg), diesel (45.6 MJ/kg), and sustainable aviation fuel (SAF, 43–48 MJ/kg). These values represent the intrinsic gravimetric energy densities of fuels and are substantially higher than the practical cell- or pack-level specific energies of lithium-ion batteries (0.36-0.95 MJ/kg), highlighting the high mass-based energy-carrying capability of hydrocarbons for transportation applications. Complete system-level comparisons require additional considerations, including storage infrastructure, conversion efficiency, and auxiliary

Just Accepted

components. Additionally, hydrocarbons offer advantages in power output capacity and long-term storage stability—up to several decades (Fig. 8b).

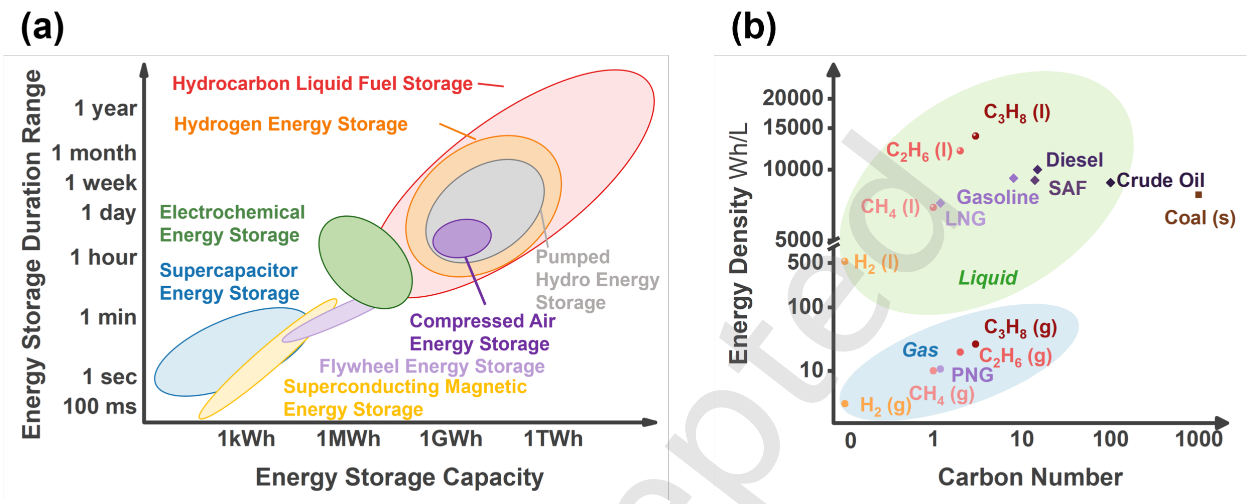

Fig. 8. Comparative properties of widely used energy-dense hydrocarbon compounds. (**a**) Storage duration versus capacity for various storage technologies. (**b**) Volumetric energy density of energy carriers as a function of carbon number.

These characteristics endow liquid fuels with irreplaceable advantages in system economics, temporal stability, and spatial flexibility, despite rapid advances in electricity and hydrogen. Hydrocarbon liquid fuels feature low production costs, high energy density, and low storage and transportation costs, supported by comprehensive infrastructure (Table 1). However, traditional production pathways—relying heavily on fossil fuels and generating high carbon emissions—constrain their long-term viability. Developing sustainable, low-carbon production pathways for liquid fuels is therefore crucial.

The Global Energy Interconnection Development and Cooperation Organization (GEIDCO) forecasts that electricity consumption for power-to-hydrogen and other power-to-fuel technologies will reach 2,000 TWh and 2,800 TWh by 2050 and 2060, respectively, accounting for 13% and 16% of total global electricity demand (Fig. 9a)[59]. In mobile energy supply sectors like aviation, shipping, and heavy transportation, liquid fuels remain difficult to replace directly with electrochemical storage or hydrogen. For example, achieving over 80% reduction in life-cycle carbon emissions and contributing to 60% of the global aviation industry's carbon reduction target by 2050 will likely depend on SAF (Fig. 9b) [60].

Just Accepted

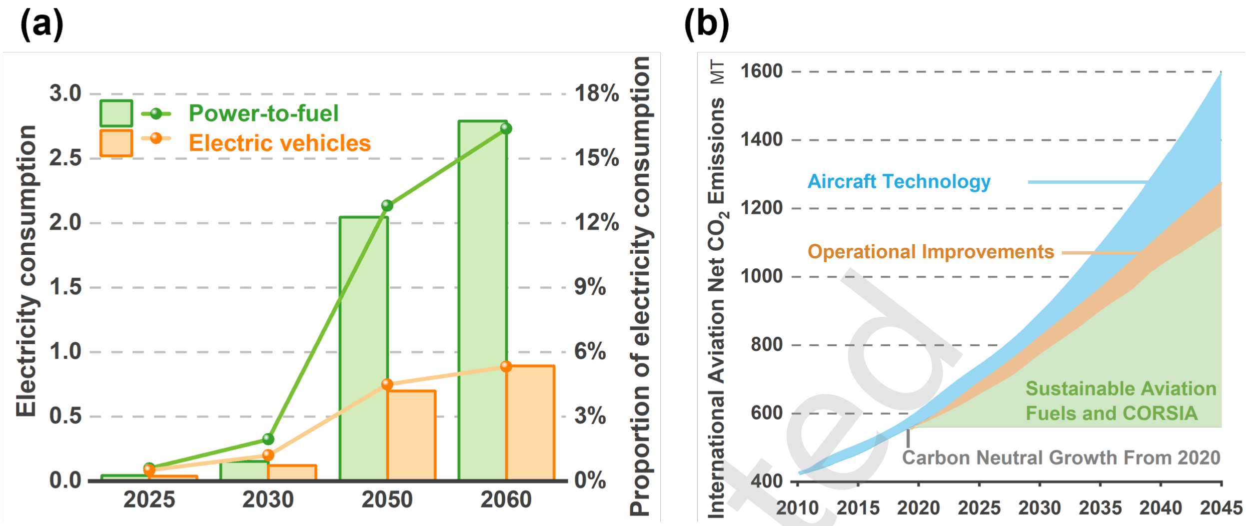

Fig. 9. The Irreplaceability of Liquid Fuels. (**a**) Comparative analysis of hydrocarbon liquids, hydrogen, and electricity as energy carriers across production cost, energy density, storage cost, transportation cost, and infrastructure requirements. (**b**) Contribution of sustainable aviation fuel (SAF) to carbon emission reduction in the aviation sector.

Just Accepted

Table 1: Comparison of Energy Carriers and Their Infrastructure in China

Indicator	Liquid Fuels				Hydrogen		Electricity	
	Gasoline	Diesel	Biodiesel	SAF	Cryogenic Liquid Hydrogen	High-Pressure Gaseous Hydrogen	Power Transmission	Battery
Production Cost (CNY/kg)	8.5-9.5	6.5-7.6	9	16-20	20-40/kg		——	
Production Cost (CNY/kWh)	~0.7	~5.5	~0.85	~1.5	0.6-1.2		0.2-0.3	
Mass Energy Density (kWh/kg)	12.2	12.6-12.8	10.5-10.8	11.9-12.2	33.3		0.15-0.35	
Volumetric Energy Density (MJ/L)	31-32	35.8-36	32-33	35.2	8.6	4.8(700bar)	——	
Storage	Tank Maintenance: 0.1 CNY/ton/day				7.9-19.2 CNY/kg (-253°C)		——	
Transportation Distance	Long Distance (1000+ km): Pipeline, Tanker, Railway				Medium-Long Distance (>500 km): Liquid Hydrogen or Pipeline	Short Distance	Long Distance: 2000-3000 km, Ultra-High Voltage Transmission	Short Distance (<500 km)
Transportation Cost	Road Transport: 0.3-0.5 CNY/ton·km Maritime Transport Cost: 0.1 CNY/ton·km				28-34 CNY/ton·km	500km:＞20 CNY/kg	＜0.01 CNY/kWh·1000 km	Affected by Battery Life,
Existing Infrastructure	• Over 100,000 gas stations • About 26,000 km of crude oil pipelines, with a mature storage and transportation system.				• Over 540 hydrogen refueling stations • 400 km pure hydrogen pipelines ,with most hydrogen pipeline transportation still in the demonstration stage. • High energy consumption for liquid hydrogen		• Over 18.5 million charging piles • 40 lines, including 20 AC and 20 DC lines, with a total length of about 54,000 km • The construction cost of ultra-high voltage is high (over 20 billion CNY per line).	

Just Accepted

Low-carbon hydrocarbon production pathways can be categorized into two main types based on carbon sources: biomass synthesis and sunlight to fuel(STF) synthesis. Biomass synthesis converts organic waste into fuels through various processes, including anaerobic digestion (methane production), gasification (e.g., biomass-to-methanol)[61-63], transesterification (biodiesel)[64-66], or pyrolysis (bio-crude oil)[67, 68]. These processes can reduce carbon emissions by 60-90%. Global biodiesel annual production has increased from 16 million tons in 2010 to 76.3 million tons in 2024 (Fig. 10a)[69]. However, further development faces significant constraints from feedstock supply limitations (competition with food crops for arable land and uneven distribution), conversion efficiency challenges, and economic viability concerns.

An alternative approach is Sunlight to Fuel (STF), which combines carbon capture technologies with artificial rapid deoxygenation processes and precise carbon–carbon coupling. This method stores clean energy as chemical energy in hydrocarbons. When these synthetic fuels combust, they release the same amount of CO_2 captured during production, theoretically achieving zero lifecycle carbon emissions. This artificial rapid deoxygenation pathway would help balance carbon cycle disruption caused by massive human energy consumption, creating a new fast-cycling equilibrium.

This approach utilizes renewable electricity from photovoltaics, wind power, and the promising solar-thermal/ultra-supercritical(with prospective higher-efficiency) power generation for water electrolysis to produce hydrogen. Concurrently, it employs CO_2 from industrial point sources, biomass, and future direct air capture as carbon feedstock. Through CO_2 hydrogenation, solar energy is stored chemically within synthetic renewable fuels (Fig. 11). Different hydrogenation products require varying hydrogen consumption (Fig. 10b), enabling different levels of hydrogen utilization and addressing storage and transportation challenges for various clean energy sources. This reaction approach has rapidly gained significant attention, with researchers implementing it through photo-, electro-, or thermos-catalysis[70-73].

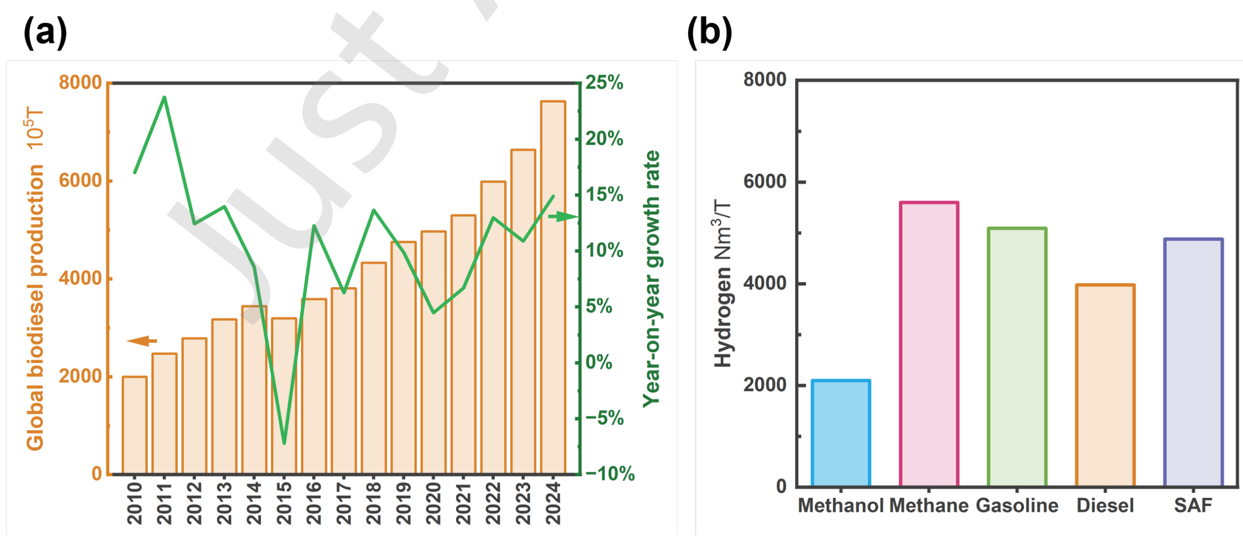

Fig. 10. (**a**) Annual global biodiesel production volumes. (**b**) Theoretical hydrogen consumption requirements for different products.

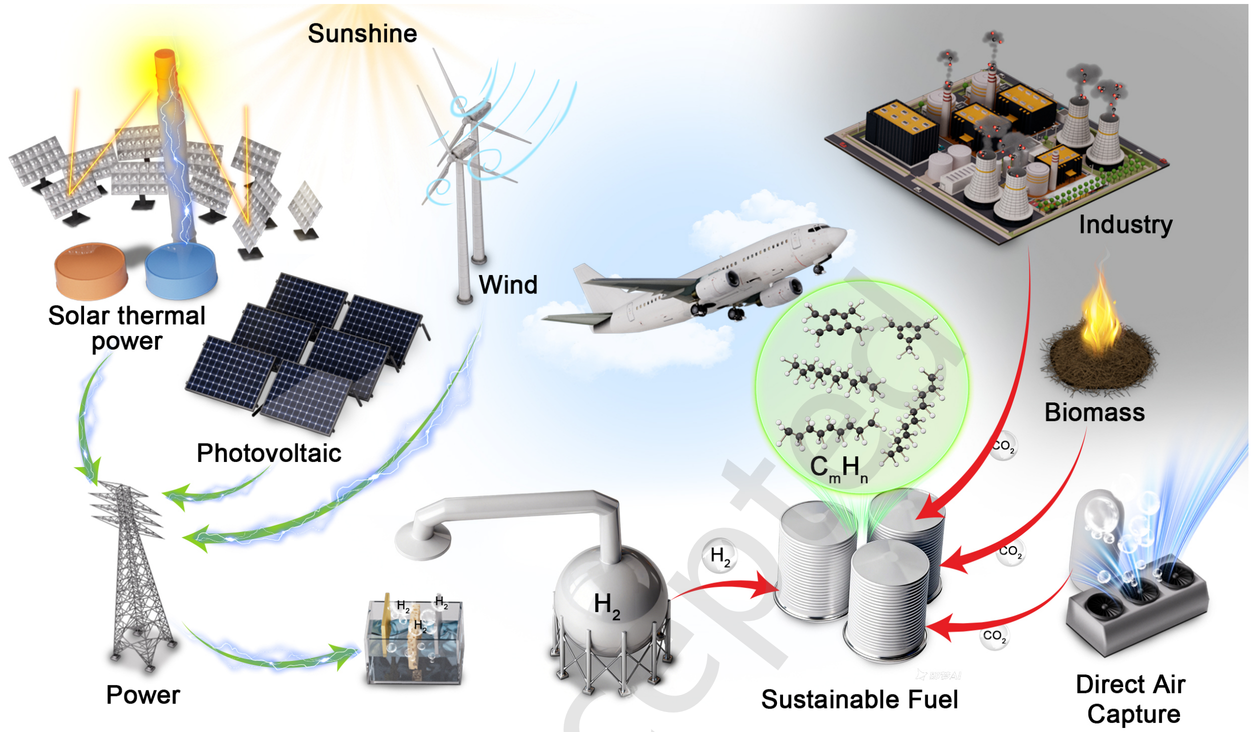

Fig.11 Schematic illustration of the integrated process for converting sunlight into sustainable hydrocarbon fuels.

3.2 Sustainable carbon-cycle fuel

Among these approaches, thermos-catalysis represents industrially advanced and technologically mature direction for converting CO_2 to liquid fuels through hydrogenation, primarily utilizing catalysts under high-temperature and high-pressure conditions[74-76]. Based on this technology, we propose the concept of "sustainable carbon-cycle fuel".

Sustainable carbon-cycle fuels provide a promising strategy to simultaneously address two key challenges in future energy systems: the utilization of renewable energy and the recycling of anthropogenic CO_2. By converting intermittent renewable electricity into stable chemical energy carriers while consuming CO_2 as a carbon feedstock, this pathway offers a potential route for long-term energy storage and carbon circulation. In recent years, extensive studies have investigated CO_2 hydrogenation using renewable H_2, with major advances in catalyst development, reaction mechanisms, and product selectivity control. These catalyst innovations, including improved active-site regulation, catalyst–support interactions, and tandem catalytic architectures, have substantially enhanced CO_2 conversion efficiency, product selectivity, and resistance to deactivation. Beyond these catalytic advances, we envision that the deeper significance of this pathway lies in its ability to integrate sequential chemical transformations at the catalyst level. Through rational catalyst coupling and controlled molecular transfer between catalytic domains, multiple reaction steps can be organized into an integrated molecular-scale conversion network, resembling the spatially coupled yet functionally coordinated energy conversion processes in

Just Accepted

biological systems. This perspective provides new inspiration for designing future carbon-cycle energy systems.

The complete CO_2 hydrogenation process demonstrates remarkable thermodynamic and functional parallels with natural photosynthesis (Fig. 12). Photosynthesis uses CO_2, H_2O, and light energy as inputs, coupling light reactions (water splitting and ATP/NADPH generation on thylakoid membranes) with dark reactions (Calvin cycle in chloroplast stroma) to achieve carbon fixation and produce organic compounds such as glucose. Similarly, CO_2 hydrogenation systems use CO_2 and H_2 (derived from renewable energy-powered water electrolysis) as raw materials. Through "light–electric–thermal" multi-energy coupled catalysis, these systems reduce CO_2 to methanol, aromatics, or long-chain hydrocarbon fuels. Both processes utilize CO_2 as a carbon source and H_2O as a hydrogen source (directly or indirectly), converting light or electrical energy into chemical energy stored in C–H bonds, thus completing the deoxygenation and reconstruction phases of the carbon cycle.

Furthermore, modular energy conversion pathways in both systems show striking similarities. Green hydrogen production through clean energy and water electrolysis corresponds to thylakoid membrane light reactions, simultaneously achieving water deoxygenation and energy form conversion. Meanwhile, catalyst-mediated CO_2 hydrogenation parallels photosynthetic dark reactions by forming reaction cycles (Calvin cycle in photosynthesis; aromatic cycle, phenol cycle, and aldol cycle triple coupling in artificial systems) to achieve target product enrichment through selective and functional regulation.[77-79]

This artificial CO_2 synthesis pathway significantly enhances solar-to-chemical energy conversion efficiency. Due to improvements in water electrolysis and photovoltaic conversion, current photovoltaic technologies achieve solar-to-electricity conversion efficiencies of approximately 20-25% at the commercial module level, while advanced tandem and multijunction solar cells can exceed 30%[80]. The electricity-to-hydrogen efficiency of industrial water electrolysis typically ranges from ~60-80%, with advanced systems approaching higher efficiencies[81]. Under optimized catalytic conditions, CO_2 hydrogenation can achieve energy conversion efficiencies of approximately 80%. Based on these component-level efficiencies, the integrated solar-to-chemical conversion efficiency of this pathway could theoretically approach approximately 16%, representing an advanced upper-bound scenario rather than current industrial performance. Nevertheless, this projected efficiency exceeds the upper range reported for natural photosynthesis (~1–7%) [82], highlighting the potential of artificial carbon-cycle pathways for highly efficient renewable energy storage. Moreover, the fundamentally different mechanisms of water consumption result in a substantial disparity in their water use efficiency. In photosynthesis, transpirational water loss dominates (~97-99%)[83], driven by the unavoidable coupling between CO_2 uptake and water vapor loss through stomata. Only ~1-3% of absorbed water participates in photolytic reactions[84]. In contrast, the artificial CO_2 synthesis pathway employs water exclusively as a chemical feedstock for electrolytic hydrogen production, with reaction-generated water recoverable for recycling. This mechanistic distinction-eliminating transpirational losses entirely-accounts for the over two orders of improvement in water use efficiency.

Similar processes have been extensively researched domestically and internationally. Our team at Tsinghua University has completed hundred-ton-scale pilot verification of green CO_2

Just Accepted

hydrogenation conversion technology. On May 6, 2022, the inauguration ceremony for the world's first 10,000-ton industrial demonstration project for CO_2 hydrogenation was held in Ordos, Inner Mongolia[54, 85]. Furthermore, in 2025, we completed the construction and operational validation of a hundred-ton-scale pilot facility in Ordos and a kiloton-scale demonstration project in Meishan, Sichuan, providing further engineering evidence for the scalability and practical feasibility of this technology.

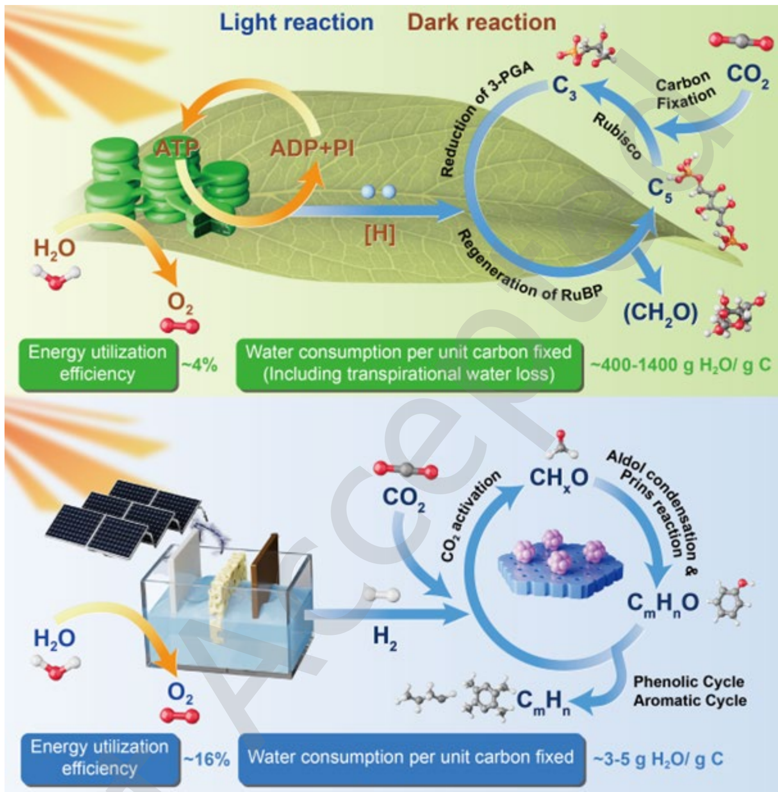

Fig. 12. Thermodynamic and functional parallels between CO_2 hydrogenation for carbon-cycle fuel production and natural photosynthetic processes.

4. Conclusions and Suggestions

In the context of the current energy transition, renewable power generation has achieved significant advantages over coal-fired power in both cost and carbon emission intensity, laying an economic and environmental foundation for large-scale deployment. Concurrently, advances in water electrolysis technology have positioned hydrogen as a highly competitive large-scale energy storage carrier. However, green hydrogen production depends entirely on green electricity, while mainstream technologies such as wind and photovoltaic power remain constrained by the intermittent nature of near-surface wind and solar resources—leading to severe spatiotemporal mismatches between energy supply and demand. Developing long-duration energy storage technologies has therefore become central to advancing high-quality renewable energy development.

Against this backdrop, we emphasize the technological pathway of synthesizing liquid fuels via CO_2 reduction using electrolysis-derived green hydrogen—the "solar-to-liquid fuels" route. This

Just Accepted

pathway converts intermittent renewable energy into liquid fuels suitable for long-term storage and cross-regional transportation, fundamentally addressing spatiotemporal mismatch challenges. Moreover, the resulting products are highly compatible with existing refining, storage, transportation, and utilization infrastructure, offering considerable industrial cost advantages and enabling smooth fossil fuel substitution.

Notably, the energy conversion efficiency of this artificial synthesis pathway is projected to be 4–10 times higher than natural photosynthesis, while water utilization efficiency improves by over two orders of magnitude. This substantial advantage creates engineering possibilities for establishing fossil fuel-independent energy systems in vast, water-scarce regions such as deserts and the Gobi, indicating exceptionally broad development prospects.

To date, this pathway has achieved promising progress in laboratory research and preliminary industrial demonstrations. However, realizing large-scale commercialization still requires addressing several key challenges. Recent advances in catalyst engineering have significantly improved CO_2 hydrogenation activity, selectivity, and stability[85-88]; however, maintaining long-term catalytic performance under industrially relevant conditions while simultaneously achieving high efficiency and economic viability remains an important challenge.

Beyond core technical hurdles related to rapid deoxygenation and precise catalysis, the sustainable sourcing of CO_2 represents another critical challenge for carbon-cycle fuel synthesis. Although DAC and CCUS technologies provide promising approaches for supplying carbon feedstocks, their large-scale deployment may introduce additional energy consumption, water requirements, material demands, and economic burdens, which should be carefully considered to ensure net carbon benefits. Integrating CO_2 capture processes with renewable energy, developing low-energy and recyclable capture materials, utilizing low-carbon process heat, and conducting comprehensive life-cycle assessments will be essential for minimizing these potential environmental impacts. Together, these strategies will be critical for realizing truly sustainable carbon-cycle fuel systems by ensuring efficient carbon recycling and minimizing environmental burdens across the entire energy conversion pathway.

Translating these technological advances into industrial deployment will also require supportive policy frameworks and market mechanisms. Global carbon neutrality initiatives are increasingly creating favorable conditions for low-carbon fuel deployment. For example, global initiatives including the European Union’s ReFuelEU Aviation Regulation, the United States Sustainable Aviation Fuel Grand Challenge and clean fuel incentives under the Inflation Reduction Act, as well as China’s carbon neutrality strategy and emerging sustainable aviation fuel development initiatives, are creating supportive policy environments for the deployment of low-carbon and synthetic fuels. Continued alignment between technological innovation, carbon markets, and fuel

Just Accepted

policies will be critical for enabling large-scale carbon recycling and accelerating the transition from fossil-based fuels toward sustainable carbon-cycle energy systems.

Despite these challenges, this pathway represents a pivotal direction for fundamentally resolving renewable energy's spatiotemporal mismatch and achieving complete fossil fuel substitution. Technological breakthroughs and engineering progress in this area are expected to profoundly impact the global transition toward carbon-neutral energy systems.

Just Accepted

References:

[1] D. Archer, The global carbon cycle, Princeton University Press, Princeton, America, 2011.

[2] W. M. Post, T.-H. Peng, W. R. Emanuel, A. W. King, V. H. Dale, D. L. DeAngelis, The global carbon cycle, *American Scientist*, 78(4)(1990)310-326.

[3] D. S. Schimel, Terrestrial ecosystems and the carbon cycle, *Global change biology*, 1(1)(1995)77-91.

[4] C. B. Field, M. J. Behrenfeld, J. T. Randerson, P. Falkowski, Primary production of the biosphere: integrating terrestrial and oceanic components, *Science*, 281(5374)(1998)237-240.

[5] W. H. Schlesinger, J. A. Andrews, Soil respiration and the global carbon cycle, *Biogeochemistry*, 48(1)(2000)7-20.

[6] R. Dasgupta, M. M. Hirschmann, The deep carbon cycle and melting in Earth's interior, *Earth and Planetary Science Letters*, 298(1-2)(2010)1-13.

[7] A. Buob, R. W. Luth, M. W. Schmidt, P. Ulmer, Experiments on $CaCO_3$-$MgCO_3$ solid solutions at high pressure and temperature, *American Mineralogist*, 91(2-3)(2006)435-440.

[8] P. Falkowski, R. J. Scholes, E. Boyle, J. Canadell, D. Canfield, J. Elser, N. Gruber, K. Hibbard, P. Högberg, S. Linder, The global carbon cycle: a test of our knowledge of earth as a system, *Science*, 290(5490)(2000)291-296.

[9] P. Friedlingstein, M. W. Jones, M. O'sullivan, R. M. Andrew, J. Hauck, G. P. Peters, W. Peters, J. Pongratz, S. Sitch, C. Le Quéré, Global carbon budget 2019, *Earth Syst. Sci. Data*, 11(4)(2019)1783-1838.

[10] P. Friedlingstein, M. O'Sullivan, M. W. Jones, R. M. Andrew, J. Hauck, P. Landschützer, C. Le Quéré, H. Li, I. T. Luijkx, A. Olsen, et al., Global Carbon Budget 2024, *Earth Syst. Sci. Data*, 17(3)(2025)965-1039.

[11] H. Ritchie, P. Rosado, M. Roser, CO_2 and Greenhouse Gas Emissions, Our World in Data, 2023 [2024-11-21], https://ourworldindata.org/co2-and-greenhouse-gas-emissions.

[12] X. Lan, P. Tans, K. W. Thoning, Trends in globally-averaged CO_2 determined from NOAA Global Monitoring Laboratory measurements, NOAA Global Monitoring Laboratory, 2025 [2025-04-14], https://doi.org/10.15138/9N0H-ZH07.

[13] Global Climate Highlights 2024, 2025 https://climate.copernicus.eu/global-climate-highlights-2024.

[14] European Commission, Delivering the European Green Deal: On the path to a climate-neutral Europe by 2050, European Commission, 2023 [2025-04-10], https://commission.europa.eu/strategy-and-policy/priorities-2019-2024/european-green-deal/delivering-european-green-deal_en.

[15] Climate Action Tracker, 2100 Warming Projections: Emissions and expected warming based on pledges and current policies., Climate Analytics and NewClimate Institute, 2024 https://climateactiontracker.org/global/temperatures/.

[16] IEA, Electricity 2025, CC BY 4.0, 2025 [2024-02], https://www.iea.org/reports/electricity-2025.

[17] IRENA, Renewable capacity statistics 2025, International Renewable Energy Agency, 978-92-9260-652-7, 2025 [2025-03], **https://www.irena.org/Publications/2025/Mar/Renewable-capacity-statistics-2025**.

[18] IEA, Renewables 2023, CC BY 4.0, 2024 [2024-01-11], https://www.iea.org/reports/renewables-2023.

[19] IEA, Global Energy Review 2025, CC BY 4.0, 2025 [2025-03], https://www.iea.org/reports/global-energy-review-2025.

[20] National Energy Administration, National Energy Administration Releases 2024 National Power Industry Statistical Data, National Energy Administration, 2025 [2025-01-21], https://www.nea.gov.cn/20250121/097bfd7c1cd3498897639857d86d5dac/c.html.

[21] N. B. o. S. o. China, Statistical Communiqué of the People's Republic of China on the 2024 National Economic and Social Development, National Bureau of Statistics of China, 2025 [2025-02-28], https://www.stats.gov.cn/sj/zxfb/202502/t20250228_1958817.html.

[22] M. A. Green, The passivated emitter and rear cell (PERC): From conception to mass production, *Solar Energy*

Materials and Solar Cells, 143(2015)190-197.
[23] A. Blakers, Development of the PERC solar cell, *IEEE Journal of Photovoltaics*, 9(3)(2019)629-635.
[24] B. Kafle, B. S. Goraya, S. Mack, F. Feldmann, S. Nold, J. Rentsch, TOPCon–technology options for cost efficient industrial manufacturing, *Solar Energy Materials and Solar Cells*, 227(2021)111100.
[25] L. Wang, Y. Tang, S. Zhang, F. Wang, J. Wang, Energy yield analysis of different bifacial PV (photovoltaic) technologies: TOPCon, HJT, PERC in Hainan, *Solar Energy*, 238(2022)258-263.
[26] S. De Wolf, A. Descoeudres, Z. C. Holman, C. Ballif, High-efficiency silicon heterojunction solar cells: A review, *green*, 2(1)(2012)7-24.
[27] M. C. Scharber, N. S. Sariciftci, Efficiency of bulk-heterojunction organic solar cells, *Progress in polymer science*, 38(12)(2013)1929-1940.
[28] IEA, Evolution of solar PV module cost by data source, 1970-2020, IEA, CC BY 4.0, 2020 [2020-07-02], https://www.iea.org/data-and-statistics/charts/evolution-of-solar-pv-module-cost-by-data-source-1970-2020.
[29] A. M. Elshurafa, S. R. Albardi, S. Bigerna, C. A. Bollino, Estimating the learning curve of solar PV balance–of–system for over 20 countries: Implications and policy recommendations, *Journal of Cleaner Production*, 196(2018)122-134.
[30] G. F. Nemet, Beyond the learning curve: factors influencing cost reductions in photovoltaics, *Energy policy*, 34(17)(2006)3218-3232.
[31] Lazard, Lazard's Levelized Cost of Energy + June 2024, Lazard, 2024 [2024-06], https://www.lazard.com/media/xemfey0k/lazards-lcoeplus-june-2024-_vf.pdf.
[32] M. Bolinger, R. Wiser, E. O'Shaughnessy, Levelized cost-based learning analysis of utility-scale wind and solar in the United States, *Iscience*, 25(6)(2022)
[33] Renewable Energy Editorial, Breaking News! An Analysis of the Current Situation of the Levelized Cost of Energy (LCOE) for Photovoltaic Power Generation in 2024!, Toutiao, 2024 [2024-03-27], https://www.toutiao.com/article/7350836236627509795/.
[34] IRENA, Renewable Power Generation Costs in 2023, International Renewable Energy Agency, 978-92-9260-621-3, 2024 [2024-09], https://www.irena.org/Publications/2024/Sep/Renewable-Power-Generation-Costs-in-2023-ZH.
[35] X. Jin, Review of China's Power Development in 2024 and Outlook for 2025, China Society for Hydropower Engineering, 2025 [2023-03-03], http://www.hydropower.org.cn/cn/index/734_37717_122322.
[36] China Meteorological Administration, Annual Report on China's Wind and Solar Energy Resources in 2024, China Meteorological Administration, 2025 [2025-02-11], https://www.cma.gov.cn/zfxxgk/gknr/qxbg/202502/t20250211_6847016.html.
[37] IEA, The California Duck Curve, IEA, CC BY 4.0, 2019 [2019-10-9], https://www.iea.org/data-and-statistics/charts/the-california-duck-curve.
[38] Denholm P, O'Connell M, Brinkman G, Jorgenson J. Overgeneration from solar energy in California: A field guide to the duck chart[R]. Golden, CO: National Renewable Energy Laboratory, 2015.
[39] Engaging Data. California Electricity Generation. 2025. Available at: https://engaging-data.com/california-electricity-generation/?date=2025-10-26
[40] X. Du, Z. Lang, M. Liu, J. Wu, Regression analysis and prediction of monthly wind and solar power generation in China, *Energy Reports*, 12(2024)1385-1402.
[41] Y. Wang, R. Wang, K. Tanaka, P. Ciais, J. Penuelas, Y. Balkanski, J. Sardans, D. Hauglustaine, W. Liu, X. Xing, Accelerating the energy transition towards photovoltaic and wind in China, *Nature*, 619(7971)(2023)761-767.
[42] National Energy Administration, Construction Situation of Photovoltaic Power Generation in 2024, National Energy Administration, 2025 [2025-01-27], https://www.nea.gov.cn/20250221/f04452701c914d51a89d0c0ea6f4acd1/c.html.
[43] R. Idel, Levelized full system costs of electricity, *Energy*, 259(2022)124905.
[44] F. Ueckerdt, L. Hirth, G. Luderer, O. Edenhofer, System LCOE: What are the costs of variable renewables?, *Energy*, 63(2013)61-75.
[45] S. Chong, J. Wu, I.-S. Chang, Cost accounting and economic competitiveness evaluation of photovoltaic power generation in China——based on the system levelized cost of electricity, *Renewable Energy*, 222(2024)119940.
[46] H. Jiang, L. Yao, J. Qin, Y. Bai, M. Brandt, X. Lian, S. J. Davis, N. Lu, W. Zhao, T. Liu, Globally interconnected solar-wind system addresses future electricity demands, *Nature Communications*, 16(1)(2025)4523.
[47] K. Marvel, B. Kravitz, K. Caldeira, Geophysical limits to global wind power, *Nature Climate Change*, 3(2)(2013)118-121.

Just Accepted

[48] A. Ajanovic, M. Sayer, R. Haas, The economics and the environmental benignity of different colors of hydrogen, *International Journal of Hydrogen Energy*, 47(57)(2022)24136-24154.
[49] IEA, Global Hydrogen Review 2024, IEA, CC BY 4.0, 2024 [2024-10], https://www.iea.org/reports/global-hydrogen-review-2024.
[50] Hydrogen Council,McKinsey & Company, Hydrogen for Net-Zero: A critical cost-competitive energy vector, Hydrogen Council, 2021 [2021-11], https://hydrogencouncil.com/wp-content/uploads/2021/11/Hydrogen-for-Net-Zero.pdf.
[51] F. Pavan, J. M. Bermudez, A. Pizarro, U. Remme, H. Blanco, Electrolysers, IEA, CC BY 4.0, 2025 [2025-02-25], https://www.iea.org/energy-system/low-emission-fuels/electrolysers.
[52] Yinchuang Think Tank, Development Map of China's Hydrogen Energy Industry: Hydrogen Production, Storage and Transportation, and Applications (2024 Edition), Xueqiu, 2024 [2024-06-12], https://xueqiu.com/9615908983/293537022.
[53] R. Bocca, W. Liu, H. Zhu, Green Hydrogen Acceleration Initiative - White Paper on Recommendations for Empowering Measures of Green Hydrogen in China, World Economic Forum, 2023 [2023-08], https://www3.weforum.org/docs/WEF_Green_Hydrogen_in_China_A_Roadmap_for_Progress_2023_CN.pdf.
[54] G. Tian, C. Zhang, F. Wei, Fueling the future: Innovating the path to carbon-neutral skies with CO_2-to-aviation fuel, *Carbon Future*, 1(2)(2024)9200010-9200011-9200010-9200011.
[55] S. Krishnan, V. Koning, M. T. de Groot, A. de Groot, P. G. Mendoza, M. Junginger, G. J. Kramer, Present and future cost of alkaline and PEM electrolyser stacks, *International journal of hydrogen energy*, 48(83)(2023)32313-32330.
[56] M. T. Zun, B. C. McLellan, Cost projection of global green hydrogen production scenarios, *Hydrogen*, 4(4)(2023)932-960.
[57] 闫喻婷, 氢气储运方式的经济性对比研究, 华中科技大学, 2021.
[58] H. Ibrahim, A. Ilinca, J. Perron, Energy storage systems—Characteristics and comparisons, *Renewable and sustainable energy reviews*, 12(5)(2008)1221-1250.
[59] Global Zero Carbon, A critical data shift reveals China's new trends in carbon neutrality, 2023 [2023-02-22], https://www.chinacace.org/news/fieldsview?id=14440#.
[60] ICAO, Climate Change, ICAO, 2022 https://www.icao.int/environmental-protection/Pages/climate-change.aspx.
[61] S. Shabangu, D. Woolf, E. M. Fisher, L. T. Angenent, J. Lehmann, Techno-economic assessment of biomass slow pyrolysis into different biochar and methanol concepts, *Fuel*, 117(2014)742-748.
[62] C. N. Hamelinck, A. P. Faaij, Future prospects for production of methanol and hydrogen from biomass, *Journal of Power sources*, 111(1)(2002)1-22.
[63] M. L. G. Renó, E. E. S. Lora, J. C. E. Palacio, O. J. Venturini, J. Buchgeister, O. Almazan, A LCA (life cycle assessment) of the methanol production from sugarcane bagasse, *Energy*, 36(6)(2011)3716-3726.
[64] H. Fukuda, A. Kondo, H. Noda, Biodiesel fuel production by transesterification of oils, *Journal of bioscience and bioengineering*, 92(5)(2001)405-416.
[65] D. Y. Leung, X. Wu, M. K. H. Leung, A review on biodiesel production using catalyzed transesterification, *Applied energy*, 87(4)(2010)1083-1095.
[66] L. C. Meher, D. V. Sagar, S. N. Naik, Technical aspects of biodiesel production by transesterification—a review, *Renewable and sustainable energy reviews*, 10(3)(2006)248-268.
[67] V. Yakovlev, S. Khromova, O. Sherstyuk, V. Dundich, D. Y. Ermakov, V. Novopashina, M. Y. Lebedev, O. Bulavchenko, V. Parmon, Development of new catalytic systems for upgraded bio-fuels production from bio-crude-oil and biodiesel, *Catalysis Today*, 144(3-4)(2009)362-366.
[68] K. Wang, D. C. Dayton, J. E. Peters, O. D. Mante, Reactive catalytic fast pyrolysis of biomass to produce high-quality bio-crude, *Green Chemistry*, 19(14)(2017)3243-3251.
[69] World Bioenergy Association, Global Bioenergy Statistics Report 2024, World Bioenergy Association, 2024 https://www.worldbioenergy.org/uploads/241023%20GBS%20Report%20Short%20Version.pdf.
[70] T. Kong, Y. Jiang, Y. Xiong, Photocatalytic CO_2 conversion: What can we learn from conventional CO_x hydrogenation?, *Chemical Society Reviews*, 49(18)(2020)6579-6591.
[71] W.-H. Wang, Y. Himeda, J. T. Muckerman, G. F. Manbeck, E. Fujita, CO_2 hydrogenation to formate and methanol as an alternative to photo-and electrochemical CO_2 reduction, *Chemical reviews*, 115(23)(2015)12936-12973.
[72] D. Miao, Y. Ding, T. Yu, J. Li, X. Pan, X. Bao, Selective synthesis of benzene, toluene, and xylenes from syngas, *ACS Catalysis*, 10(13)(2020)7389-7397.
[73] J. Yang, X. Pan, F. Jiao, J. Li, X. Bao, Direct conversion of syngas to aromatics, *Chemical communications*,

53(81)(2017)11146-11149.
[74] Y. Wang, W. Gao, S. Kazumi, H. Li, G. Yang, N. Tsubaki, Direct and oriented conversion of CO2 into value-added aromatics, *Chemistry–A European Journal*, 25(20)(2019)5149-5153.
[75] B. Zhao, P. Zhai, P. Wang, J. Li, T. Li, M. Peng, M. Zhao, G. Hu, Y. Yang, Y.-W. Li, Direct transformation of syngas to aromatics over Na-Zn-Fe5C2 and hierarchical HZSM-5 tandem catalysts, *Chem*, 3(2)(2017)323-333.
[76] K. Cheng, W. Zhou, J. Kang, S. He, S. Shi, Q. Zhang, Y. Pan, W. Wen, Y. Wang, Bifunctional catalysts for one-step conversion of syngas into aromatics with excellent selectivity and stability, *Chem*, 3(2)(2017)334-347.
[77] M. T. Arslan, B. Ali, S. Z. A. Gilani, Y. Hou, Q. Wang, D. Cai, Y. Wang, F. Wei, Selective conversion of syngas into tetramethylbenzene via an aldol-aromatic mechanism, *ACS Catalysis*, 10(4)(2020)2477-2488.
[78] M. T. Arslan, B. A. Qureshi, S. A. Gilani, D. Cai, Y. Ma, M. Usman, X. Chen, Y. Wang, F. Wei, Single-step conversion of H2-deficient syngas into high yield of tetramethylbenzene, *ACS Catalysis*, 9(3)(2019)2203-2212.
[79] G. Tian, X. Liang, H. Xiong, C. Zhang, F. Wei, A perspective of CO x conversion to aromatics, *EES Catalysis*, 1(5)(2023)677-686.
[80] M. A. Green, E. D. Dunlop, M. Yoshita, N. Kopidakis, K. Bothe, G. Siefer, D. Hinken, M. Rauer, J. Hohl-Ebinger, X. Hao, Solar cell efficiency tables (Version 64), *Progress in photovoltaics: research and applications*, 32(7)(2024)425-441.
[81] D. Singh, N. K. Singh, A. K. Sharma, Water electrolysis technologies for producing hydrogen: A review, *Journal of Renewable and Sustainable Energy*, 17(5)(2025)
[82] R. E. Blankenship, D. M. Tiede, J. Barber, G. W. Brudvig, G. Fleming, M. Ghirardi, M. Gunner, W. Junge, D. M. Kramer, A. Melis, Comparing photosynthetic and photovoltaic efficiencies and recognizing the potential for improvement, *science*, 332(6031)(2011)805-809.
[83] L. Taiz, I. M. Møller, A. Murphy, E. Zeiger, Plant physiology and development, *(No Title)*, 2023)
[84] J. Doorenbos, W. O. Pruitt, A. Aboukhaled, J. Damagnez, N. Dastane, C. Van Den Berg, P. Rijtema, O. Ashford, M. Frere, Crop water requirements, 1977)
[85] G. Tian, Z. Li, C. Zhang, X. Liu, X. Fan, K. Shen, H. Meng, N. Wang, H. Xiong, M. Zhao, Upgrading CO2 to sustainable aromatics via perovskite-mediated tandem catalysis, *Nature communications*, 15(1)(2024)3037.
[86] J. Zhou, Y. Miao, H. Ding, Y. Ren, L. Ye, B. Yue, H. He, Direct and stable hydrogenation of CO2 to aromatics over a tandem catalyst Zn0. 1Ti0. 9Ox/HZSM-5, *Iscience*, 27(7)(2024)
[87] J. Devos, A. Sajid, C. Aelbers, M. Dusselier, Parallel-consecutive CO formation during CO2 hydrogenation to olefins in a tandem ZnZrOx/SSZ-13, *ACS Sustainable Chemistry & Engineering*, 13(26)(2025)9964-9973.
[88] K. Jin, C. Wen, Q. Jiang, X. Zhuang, L. Chen, L. Ma, C. Wang, Q. Zhang, Conversion of CO2 to gasoline over tandem Fe/C and HZSM-5 catalysts, *Sustainable Energy & Fuels*, 7(5)(2023)1265-1272.

Just Accepted

Acknowledgments:

This work was financially supported by the National Key R&D Program of China (2022YFA1203301), National Natural Science Foundation of China (No. 22602003; 22238004; 22275110; 223B2205), National Postdoctoral Program for Innovative Talent, Shuimu scholar from Tsinghua University and the Key Research and Development Program of Inner Mongolia and Ordos.

Author contributions:

F.W., C.X. and H.X. conceived this project and designed the studies; X.L. performed the data collection and visualization; All authors are involved in the data analysis; X.L. wrote the manuscript with the help of others.

Competing interests:

The authors declare no competing interests.

Additional information:
Correspondence and requests for data should be addressed to F.W., C.X. and H.X.

Just Accepted